

Figure 2. ^{13}C (top trace) and ^1H (bottom trace) NMR spectra (300 MHz, 293 K) of **1** in D_2O (pD = 10.4). The chemical shift values from TSP are indicated.

mercaptoethylamine.²² The most unusual feature of the structure of the anion (Figure 1) is the cis disposition of the two D-Pen²⁻ ligands despite the presence of the two CH_3 groups on the β -carbon atom of the ligand. On steric grounds, a trans geometry is clearly the preferred one.²³ In **2**, the two L-cysteinate ligands are trans to each other.⁸ The cis geometry of D-Pen²⁻ ligands is also found in the tetranuclear heterometallic anion $[\text{Au}_2\text{Ni}_2(\text{SC}(\text{CH}_3)_2\text{CH}(\text{NH}_2)\text{COO})_4]^{2-}$ (**3**).²⁴ That coordination to the Au(I) centers is not the reason for the cis geometry of the D-Pen²⁻ ligands in **3** is evident from the present result—in **1**, the two D-Pen²⁻ ligands are cis to each other even though no bridge formation occurs. Another interesting aspect of the structure of **1** is the occurrence of the two carboxylate groups of the D-Pen²⁻ ligands on the same side of the mean coordination plane (Figure 1). This feature is also observed in the structures of **2**⁸ and **3**.²⁴ Presumably, this arrangement of the carboxylate groups allows better coordination to K^+ ions as well as effective H-bonding in the crystal lattice. The bond angles (Table III) and other metric parameters of the chelate rings in **1** are unexceptional.

Properties. The IR spectrum of **1** exhibits no band in the region 2600–2500 cm^{-1} , indicating coordination of the ligand as thiolate. That the carboxylate group of D-Pen²⁻ is not involved in coordination to nickel is suggested by the appearance of the anti-symmetric and symmetric $\nu(\text{COO}^-)$ at 1595 and 1400 cm^{-1} , respectively.⁸ The red color of the aqueous solution of **1** arises from a band at 462 nm ($\epsilon = 126 \text{ M}^{-1} \text{ cm}^{-1}$) with a shoulder at 560 nm ($\epsilon = 45 \text{ M}^{-1} \text{ cm}^{-1}$). In addition, the electronic absorption spectrum of **1** exhibits two strong charge-transfer bands with maxima at 312 nm ($3100 \text{ M}^{-1} \text{ cm}^{-1}$) and 270 nm ($14000 \text{ M}^{-1} \text{ cm}^{-1}$). Several groups^{10–12} have generated the $[\text{Ni}(\text{D-Pen})_2]^{2-}$ ion in aqueous solution and recorded the absorption spectrum in the visible region. We report the entire spectrum here for the first time. The features at 560 and 462 nm have been tentatively assigned to the $^1\text{A}_{1g} \rightarrow ^1\text{A}_{2g}$ and $^1\text{A}_{1g} \rightarrow ^1\text{B}_{1g}$ transitions, respectively, by another group.¹¹

The ^1H and ^{13}C NMR spectra of **1** in D_2O are shown in Figure 2. Assignments of the various peaks rely on area integration, APT data,²⁵ and the proton-coupled spectra. The clean and simple spectra confirm the stability of **1** in aqueous solution.

In conclusion, comment must be made on the unusual stability of the $[\text{Ni}(\text{D-Pen})_2]^{2-}$ anion in relation to the role of D-H₂Pen as an antidote for acute nickel toxicity. Unlike most square-planar

thiolato complexes of nickel, **1** in aqueous (pH 6–10), saline, or urine (pH 7.2) solution is stable over long periods of time. These solutions are quite resistant to air oxidation.²⁶ In fact, complex **1** is formed under aerobic conditions as well. When Ni^{2+} is mixed with excess (>4 equiv) D-H₂Pen in water (pH 8),²⁷ the characteristic red color is rapidly developed and the extinction coefficient of the 462-nm band reaches its maximum value of 125 within 1 min. No change in the absorption spectrum is noted over the next 24 h. The same result is obtained when the reaction mixture contains an equivalent amount of albumin.²⁸ It is known that the major Ni^{2+} -binding substance in human blood is albumin.⁷ Thus, serum nickel can be extracted with excess D-H₂Pen and complex **1** is expected to be the product of this reaction. It therefore appears that chemotherapy with high doses of D-H₂Pen could remove nickel in the form of the bis complex $[\text{Ni}(\text{D-Pen})_2]^{2-}$.

Acknowledgment. We wish to acknowledge support from the donors of the Petroleum Research Fund, administered by the American Chemical Society.

Supplementary Material Available: Computer-generated drawings of the two independent anions of **1** showing the K^+ -oxygen atom interactions and H-bonding by the water molecules and complete tables of crystal data, bond distances, bond angles, anisotropic displacement coefficients, and the H atom coordinates (8 pages); a listing of observed and calculated structure factors (19 pages). Ordering information is given on any current masthead page.

- (26) The extinction of the visible band shows less than 2% decomposition over 24 h. No decomposition is observed when the aqueous solution (pH ~7) contains 2–3 equiv of D-H₂Pen. The stability constant ($\log \beta_2$) of $[\text{Ni}(\text{D-Pen})_2]^{2-}$ has been determined in aqueous solution. The value of $\log \beta_2$ is 22.88 ± 0.14 .^{9–11,13}
- (27) The pK_a 's for the $-\text{COOH}$, $-\text{SH}$, and $-\text{NH}_2$ groups of D-H₂Pen are 1.99–2.00, 8.1, and 10.6, respectively.¹¹
- (28) In this experiment, Ni^{2+} was preincubated with an equivalent amount of albumin (24 h) before it was mixed with D-K₂Pen solution.

Contribution from the Department of Chemistry,
University of California, Davis, California 95616

A New Material with Alternating Metal–Oxide and Metal–Phosphide Layers: $\text{Ba}_2\text{Mn}_3\text{P}_2\text{O}_2$

Ned T. Stetson and Susan M. Kauzlarich*

Received February 21, 1991

With the discovery of high-temperature superconductors, there is a renewed interest in complex layered metal–oxide compounds.¹ In addition, there is a significant amount of interest in two-dimensional compounds due to their anisotropic physical properties. Our interest in the synthesis and properties of ternary transition-metal pnictide compounds² prompted our investigation of the synthesis and characterization of the novel layered oxide–pnictide compounds: $\text{A}_2\text{Mn}_3\text{X}_2\text{O}_2$ (A = Sr, Ba; X = As, Sb, Bi).³ Although the single-crystal structure of these compounds has been reported, no other physical characterizations have been performed. We have successfully modified the reaction procedure to produce pure materials for physical property measurements. In addition, the new compound $\text{Ba}_2\text{Mn}_3\text{P}_2\text{O}_2$ has been synthesized in high yield. This new compound is isostructural with the heavier group 15 (group VA) element analogues and has a unique two-dimensional structure with alternating metal–oxide and metal–phosphide layers separated by alkaline-earth-metal cations. This is one of the few examples of a solid-state compound that contains both oxygen and phosphorus atoms without direct bonding between them.⁴

The structure for these compounds is shown in Figure 1. They crystallize in the tetragonal system, $I4/mmm$ ($Z = 2$). Manganese

(22) Girling, R. L.; Amma, E. L. *Inorg. Chem.* **1967**, *6*, 2009.

(23) Indeed, a trans structure has been proposed by Martell in ref 14.

(24) Birker, P. J. M. W. L.; Verschoor, G. C. *Inorg. Chem.* **1982**, *21*, 990.

(25) Patt, S. L.; Shooley, J. N. *J. Magn. Reson.* **1982**, *46*, 535.

* To whom correspondence should be addressed.

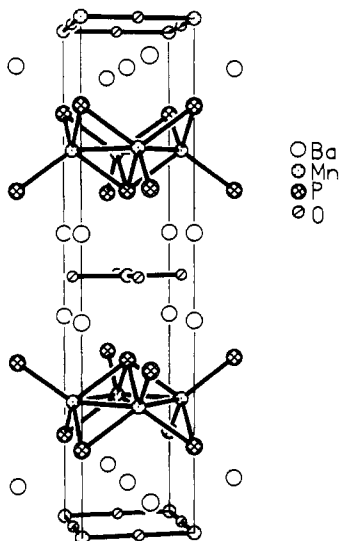


Figure 1. Structure of $\text{Ba}_2\text{Mn}_3\text{X}_2\text{O}_2$ (one unit cell shown).

atoms occupy two distinct sites. In one site, the manganese atoms are in a plane, forming the base of edge-sharing square pyramids. The phosphorus atoms cap Mn_4 squares to form pyramids alternately above and below the plane. This layer is similar to the layers found in the ThCr_2Si_2 structure type.⁵ The second manganese site is in a plane of corner-sharing $\text{MnO}_{4/2}$ squares. The two manganese layers alternate and are separated by layers of Ba or Sr cations. The oxide and pnictide atoms are in different layers separated by the alkaline-earth-metal layers and have no bonding interactions between them.

The reported synthetic method³ to prepare $\text{A}_2\text{Mn}_3\text{X}_2\text{O}_2$ (A = Sr, Ba; X = As, Sb, Bi) is to react a stoichiometric mixture of A, Mn, X, and X_2O_3 in a corundum crucible, sealed in a quartz ampule, under argon, at 1247–1397 °C. The reaction mixture was cooled at a rate of 100 °C/h. Although crystals were obtained by using this method, it has proved to be unsuccessful in producing single-phase material. We have improved the yields of these compounds as well as synthesizing the new compound, $\text{Ba}_2\text{Mn}_3\text{P}_2\text{O}_2$.

The compound $\text{Ba}_2\text{Mn}_3\text{P}_2\text{O}_2$ was synthesized by mixing stoichiometric quantities of barium oxide, ground manganese metal, and ground red phosphorus. Barium oxide was obtained by decomposing BaCO_3 (Johnson Matthey, 4N) at 1000 °C under vacuum for 48 h; manganese metal (Johnson Matthey, 3N) was cleaned with a 10% $\text{HNO}_3/\text{CH}_3\text{OH}$ solution, transferred to a drybox, and ground into a powder; and the red phosphorus (Johnson Matthey, 5N) was used as obtained. The manipulation of all reagents was carried out in a Vacuum Atmospheres drybox under an argon atmosphere (typical H_2O levels ≤ 0.1 ppm). The mixture was pressed into a pellet (ca. 0.35 kbar) and placed in a dried alumina crucible, which was sealed in a quartz ampule under 0.5 atm of purified argon. The reaction mixture was then heated at 30 °C/h to 1000 °C and held at that temperature for 1 week. The product of the reaction was a dark gray solid which retained the original pellet's shape. There was no apparent reaction with the alumina boat or the quartz ampule. This method has also been used to synthesize the previously reported $\text{A}_2\text{Mn}_3\text{X}_2\text{O}_2$

Table I. Lattice Parameters (Å) for $\text{A}_2\text{Mn}_3\text{X}_2\text{O}_2$ compounds

| compd | a^a | c^a | a^b | c^b |
|---|------------|------------|-----------|-----------|
| $\text{Sr}_2\text{Mn}_3\text{As}_2\text{O}_2$ | 4.1459 (6) | 18.856 (2) | 4.16 (1) | 18.84 (4) |
| $\text{Sr}_2\text{Mn}_3\text{Sb}_2\text{O}_2$ | 4.2599 (4) | 20.093 (3) | 4.262 (4) | 20.11 (2) |
| $\text{Sr}_2\text{Mn}_3\text{Bi}_2\text{O}_2$ | 4.2816 (6) | 20.554 (3) | 4.28 (1) | 20.55 (5) |
| $\text{Ba}_2\text{Mn}_3\text{P}_2\text{O}_2$ | 4.2029 (7) | 19.406 (5) | | |
| $\text{Ba}_2\text{Mn}_3\text{As}_2\text{O}_2$ | 4.2539 (5) | 19.755 (4) | 4.248 (5) | 19.77 (3) |
| $\text{Ba}_2\text{Mn}_3\text{Sb}_2\text{O}_2$ | 4.3650 (2) | 20.789 (2) | 4.367 (5) | 20.78 (2) |

^a This work (Guinier powder diffraction, Cu $\text{K}\alpha_1$ radiation).

^b Reference 3 (single-crystal X-ray diffraction, Mo $\text{K}\alpha$ radiation).

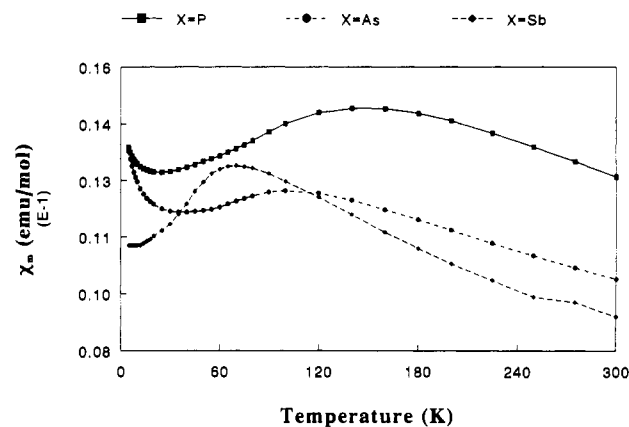


Figure 2. χ_m versus temperature (K) for $\text{Ba}_2\text{Mn}_3\text{X}_2\text{O}_2$ (X = P, As, Sb). $H = 2000$ G.

compounds in high (>80%) to quantitative yields by reacting the appropriate AO and X. The product of these reactions was a dark gray to black solid which retained the original pellet's shape. The products are moisture sensitive and slowly decompose over extended periods of exposure to air. The products were therefore handled in a nitrogen-filled drybox (typical H_2O levels ≤ 0.7 ppm), and all precautions were made to ensure minimal exposure to air. We have been unsuccessful in synthesizing either $\text{Sr}_2\text{Mn}_3\text{P}_2\text{O}_2$ or $\text{Ba}_2\text{Mn}_3\text{Bi}_2\text{O}_2$ using this method. The major products of the reactions to produce $\text{Sr}_2\text{Mn}_3\text{P}_2\text{O}_2$ are unreacted SrO and SrMn_2P_2 .⁶ The major product in the attempts to prepare the barium bismuth analogue is $\text{Ba}_2\text{Mn}_2\text{Bi}_2\text{O}_7$.

$\text{Ba}_2\text{Mn}_3\text{P}_2\text{O}_2$ was identified by Guinier X-ray powder diffraction.⁸ The 2θ values of the observed diffraction peaks were measured and corrected by a nonlinear least-squares fit of the five known silicon lines. The powder diffraction data were then indexed on the basis of the $\text{A}_2\text{Mn}_3\text{X}_2\text{O}_2$ structure type to a tetragonal cell of $a = 4.202$ (1) Å and $c = 19.406$ (5) Å.⁹ Comparisons between the line positions and intensities of the experimental diffraction pattern and a calculated pattern,¹⁰ based on the reported structure and the determined cell, give excellent agreement. These comparisons are available as supplementary material. The lattice constants for all the compounds are given in Table I. The constants for the As, Sb, and Bi analogues are in agreement with the reported single-crystal X-ray diffraction values.

Temperature-dependent magnetic measurements of the barium analogues show antiferromagnetic behavior. The magnetic susceptibility data from 6 to 300 K were measured on a Quantum Design SQUID magnetometer at 2000 G and are shown in Figure 2. The samples show broad antiferromagnetic transitions with decreasing transition temperatures and increasing pnictide size:

- (1) For reviews, see: (a) Jaeger, H. *Adv. Mater.* **1990**, *2*, 16. (b) Sleight, A. W. *Science* **1988**, *242*, 1519. (c) Santoro, A.; Beech, F.; Marezio, M.; Cava, R. J. *Physica* **1988**, *156C*, 693.
- (2) (a) Stetson, N. T.; Kauzlarich, S. M. *J. Solid State Chem.* **1991**, *91*, 140. (b) Kauzlarich, S. M. *Comments Inorg. Chem.* **1990**, *10*, 75. (c) Webb, D. J.; Kuromoto, T. K.; Kauzlarich, S. M. *J. Magn. Magn. Mater.*, in press. (d) Kuromoto, T. Y.; Webb, D. J.; Kauzlarich, S. M. *Mol. Cryst. Liq. Cryst.* **1990**, *181*, 349. (e) Kauzlarich, S. M.; Kuromoto, T. Y. *J. Am. Chem. Soc.* **1989**, *111*, 8041.
- (3) Brechtel, E.; Cordier, G.; Schäfer, H. *Z. Naturforsch.* **1979**, *34B*, 777.
- (4) (a) Benz, R.; Zachariasen, W. H. *Acta Crystallogr.* **1969**, *B25*, 294. (b) Hadenfeldt, C.; Vollert, H. O. *J. Less-Common Met.* **1988**, *144*, 143.
- (5) Mewis, A. *Z. Naturforsch.* **1980**, *35B*, 141.

- (6) Mewis, A. *Z. Naturforsch.* **1978**, *33B*, 606.
- (7) Brechtel, E.; Cordier, G.; Schäfer, H. *Z. Naturforsch.* **1981**, *36B*, 27.
- (8) An Enraf-Nonius FR 522 Guinier camera with Cu $\text{K}\alpha_1$ radiation and NBS silicon, as an internal reference, was used.
- (9) Cell parameters were obtained by indexing the powder patterns with the least-squares program LATT: Takusagawa, F.; Corbett, J. D. Iowa State University, 1981. Unpublished.
- (10) Clark, C. M.; Smith, D. K.; Johnson, G. J. A FORTRAN II Program for Calculating X-ray Diffraction Patterns-Version 5. Department of Geosciences, Pennsylvania State University, University Park, PA, 1973. Position parameters were taken from $\text{Ba}_2\text{Mn}_3\text{As}_2\text{O}_2$.³

$T_{\max} \sim 150$ K (P), 110 K (As), 60 K (Sb). These broad transitions are characteristic of low-dimensional antiferromagnetic compounds and are indicative of short-range antiferromagnetic coupling that is essentially two-dimensional above and three-dimensional below a transition temperature (T_N). This temperature (T_N) can be determined from the point of maximum slope in the temperature dependence of the magnetic susceptibility.¹¹ Points of maximum slope in the χ_m versus T curves are at temperatures ($T_N \sim 90$ K (P), 60 K (As), 50 K (Sb)) lower than the maximum temperature of the broad transition, indicating that the three-dimensional antiferromagnetic transitions will probably lie at these approximate T_N 's. The low-temperature Curie tail in the $\text{Ba}_2\text{Mn}_3\text{P}_2\text{O}_7$ and $\text{Ba}_2\text{Mn}_3\text{As}_2\text{O}_7$ samples is attributed to small amounts of paramagnetic impurities in these two samples. Above the T_{\max} , the compounds show Curie-like behavior, but lack of data above 300 K prevents a proper determination of the moment. Further magnetic studies (high-temperature magnetic susceptibility and neutron diffraction) on the barium and strontium analogues is in progress in order to better characterize the magnetic properties of these compounds. The detailed magnetic and electronic properties of these compounds will be the subject of another paper.

Acknowledgment. This research was supported in part by the National Science Foundation (Grant DMR-8913831) and the UC Davis Committee on Research. We thank Professors J. E. Greedan and D. J. Webb for useful discussions and Professor R. N. Shelton for the use of the SQUID magnetometer.

Supplementary Material Available: A table of observed and calculated X-ray powder diffraction intensity data for $\text{Ba}_2\text{Mn}_3\text{P}_2\text{O}_7$ (2 pages). Ordering information is given on any current masthead page.

- (11) (a) Navarro, R.; Smit, J. J.; de Longh, L. J.; Crama, W. J.; Ijdo, D. J. W. *Physica* 1976, 83B, 97. (b) Carlin, R. L.; van Duynveldt, A. J. *Magnetic Properties of Transition Metal Compounds*; Springer-Verlag: New York, 1977; Chapter VI.

Contribution from the Department of Chemistry, Purdue University, West Lafayette, Indiana 47907

Synthesis and Characterization of the Triply Bonded Tetrakis(cyanotrihydroborato) Complex $\text{Re}_2(\text{NCBH}_3)_4(\mu\text{-dppm})_2$

Keng-Yu Shih, Phillip E. Fanwick, and Richard A. Walton*

Received April 30, 1991

Introduction

We have demonstrated previously¹ the ability of the triply bonded dirhenium(II) complex $\text{Re}_2\text{Cl}_4(\mu\text{-dppm})_2$ ($\text{dppm} = \text{Ph}_2\text{PCH}_2\text{PPh}_2$) to react with hydride reagents such as LiAlH_4 to afford the novel polyhydride complex $\text{Re}_2\text{H}_8(\mu\text{-dppm})_2$. In a series of separate studies²⁻⁵ aimed at examining the redox behavior of $\text{Re}_2\text{Cl}_4(\mu\text{-dppm})_2$, we found that it serves as a template for the reductive coupling of nitrile ligands through the intermediacy of the dirhenium(II) nitrile-containing species $[\text{Re}_2\text{Cl}_3(\mu\text{-dppm})_2$

Table I. Crystallographic Data for $\text{Re}_2(\text{NCBH}_3)_4(\text{dppm})_2(\text{H}_2\text{O})_2 \cdot 2\text{THF}$

| | | | |
|---------------------|---|--|-----------------------------|
| chem formula | $\text{Re}_2\text{P}_4\text{O}_4\text{N}_4\text{C}_{62}\text{B}_4\text{H}_{76}$ | Z | 4 |
| fw | 1480.86 | $T, ^\circ\text{C}$ | 20 |
| space group | $C2/c$ (No. 15) | $\lambda, \text{\AA}$ | 0.71073 (Mo K α) |
| $a, \text{\AA}$ | 24.245 (3) | $\rho_{\text{calc'd}}, \text{g cm}^{-3}$ | 1.530 |
| $b, \text{\AA}$ | 18.360 (2) | $\mu(\text{Mo K}\alpha), \text{cm}^{-1}$ | 39.58 |
| $c, \text{\AA}$ | 16.450 (2) | transm coeff | 1.00-0.608 |
| β, deg | 118.618 (9) | R^a | 0.025 |
| $V, \text{\AA}^3$ | 6427 (3) | R_w^b | 0.032 |

$$^a R = \sum ||F_o| - |F_c|| / \sum |F_o|. \quad ^b R_w = \{ \sum w(|F_o| - |F_c|)^2 / \sum w|F_o|^2 \}^{1/2}; w = 1/\sigma^2(|F_o|).$$

(NCR) $_2$] $^+$. In the present report, we examine the effect of combining these disparate ligand characteristics through the use of the cyanotrihydroborato ligand $[\text{BH}_3\text{CN}]^-$. The reaction proceeds with complete $[\text{BH}_3\text{CN}]^-$ for Cl^- exchange to produce the complex $\text{Re}_2(\text{NCBH}_3)_4(\mu\text{-dppm})_2$ which has been fully characterized. This reaction course is unusual because of the large number of $[\text{BH}_3\text{CN}]^-$ ligands that have been incorporated into a single complex. Furthermore, this is the first example where the reaction of $\text{Re}_2\text{Cl}_4(\mu\text{-dppm})_2$ proceeds with complete exchange of the four chloride ligands, a clear demonstration of the remarkable stability of the $\text{Re}_2(\mu\text{-dppm})_2$ unit.

Experimental Section

Starting Materials. The complex $\text{Re}_2\text{Cl}_4(\mu\text{-dppm})_2$ was prepared according to the published method.⁷ The $\text{Na}[\text{BH}_3\text{CN}]$ reagent was purchased from Aldrich Chemical Co. All solvents were obtained from commercial sources and were deoxygenated with dinitrogen gas prior to use.

Reaction of $\text{Re}_2\text{Cl}_4(\mu\text{-dppm})_2$ with NaBH_3CN . A mixture of $\text{Re}_2\text{Cl}_4(\mu\text{-dppm})_2$ (0.20 g, 0.156 mmol) and NaBH_3CN (0.06 g, 0.955 mmol) was stirred in deoxygenated methanol (8 mL) for 6 h at room temperature. The pale green insoluble powder was filtered off and washed with methanol and diethyl ether. The crude product was extracted into 10 mL of THF, and ca. 35 mL of ethyl ether was added to the filtrate to precipitate the complex $\text{Re}_2(\text{NCBH}_3)_4(\text{dppm})_2(\text{H}_2\text{O})_2 \cdot 2\text{THF}$ as green microcrystals, yield 0.177 g (77%). Anal. Calcd for $\text{C}_{62}\text{H}_{76}\text{B}_4\text{N}_4\text{O}_4\text{P}_4\text{Re}_2$: C, 50.28; H, 5.18. Found: C, 50.22; H, 5.24. The presence of THF and water was demonstrated by ^1H NMR and IR spectroscopy and confirmed by an X-ray crystal structure determination. A batch of emerald-green crystals, which were suitable for an X-ray structure determination, were grown by the diffusion of diethyl ether vapor into a THF solution of the complex.

X-ray Structure Analysis. The structure of a crystal of composition $\text{Re}_2(\text{NCBH}_3)_4(\text{dppm})_2(\text{H}_2\text{O})_2 \cdot 2\text{THF}$ was determined by the application of standard procedures. The basic crystallographic parameters for this complex are listed in Table I. The cell constants are based on 25 reflections with $20 < \theta < 23^\circ$. Three standard reflections were measured after every 5000 s of beam exposure during data collection. Calculations were performed on a microVAX II computer using the Enraf-Nonius structure determination package. The crystal was found to belong to the monoclinic space group $C2/c$ (No. 15). Lorentz and polarization corrections were applied to the data. The structure was solved by the use of the Patterson heavy-atom method, which revealed the positions of the Re atoms of the dirhenium cation. The remaining non-hydrogen atoms were located in succeeding difference Fourier syntheses. The positions for the hydrogen atoms of the dppm ligands were calculated by assuming idealized geometry and a C-H bond distance of 0.95 Å. For the BH_3 groups of the $[\text{BH}_3\text{CN}]^-$ ligands and the uniquely determined coordinated water molecule in the asymmetric unit, one hydrogen was located in a Fourier difference map, its position was idealized, and the remaining positions were calculated. We assumed that the value of $B(\text{H})$, i.e., the isotropic equivalent thermal parameter for the hydrogen atoms, was equal to $1.3[B_{\text{eq}}(\text{C})]$ at the time of the inclusion of this parameter in the refinement procedure. While these hydrogen atoms were used in the calculation of F_o , their positions were not refined. An empirical absorption correction was used,⁸ the linear absorption coefficient being 39.58 cm^{-1} . No corrections for extinction were applied. The structures

- (1) Fanwick, P. E.; Root, D. R.; Walton, R. A. *Inorg. Chem.* 1989, 28, 3203.
 (2) Barder, T. J.; Cotton, F. A.; Falvello, L. R.; Walton, R. A. *Inorg. Chem.* 1985, 24, 1258.
 (3) Esjornson, D.; Derringer, D. R.; Fanwick, P. E.; Walton, R. A. *Inorg. Chem.* 1989, 28, 2821.
 (4) Fanwick, P. E.; Qi, J.-S.; Shih, K.-Y.; Walton, R. A. *Inorg. Chim. Acta* 1990, 172, 65.
 (5) Derringer, D. R.; Shih, K.-Y.; Fanwick, P. E.; Walton, R. A. *Polyhedron* 1991, 10, 79.

(6) Walton, R. A. *Polyhedron* 1989, 8, 1689.

(7) Cutler, A. R.; Derringer, D. R.; Fanwick, P. E.; Walton, R. A. *J. Am. Chem. Soc.* 1988, 110, 5024.

(8) Walker, N.; Stuart, D. *Acta Crystallogr., Sect. A: Found. Crystallogr.* 1983, A39, 158.